Involvement of the Arg−Asp−His Catalytic Triad in Enzymatic Cleavage of the Phosphodiester Bond†

Robert J. Kubiak,‡,§ Xiangjun Yue,‡ Robert J. Hondal,||,⊥ Cornelia Mihai,‡ Ming-Daw Tsai,|| and Karol S. Bruzik*,‡

Department of Medicinal Chemistry and Pharmacognosy, University of Illinois at Chicago, Chicago, Illinois 60612, and Departments of Chemistry and Biochemistry, The Ohio State University, Columbus, Ohio 43210

Received October 12, 2000; Revised Manuscript Received March 15, 2001

ABSTRACT: Phosphatidylinositol-specific phospholipase C (PI-PLC) catalyzes the cleavage of the P−O bond in phosphatidylinositol via intramolecular nucleophilic attack of the 2-hydroxyl group of inositol on the phosphorus atom. Our earlier stereochemical and site-directed mutagenesis studies indicated that this reaction proceeds by a mechanism similar to that of RNase A, and that the catalytic site of PI-PLC consists of three major components analogous to those observed in RNase A, the His32 general base, the His82 general acid, and Arg69 acting as a phosphate-activating residue. In addition, His32 is associated with Asp274 in forming a catalytic triad with inositol 2-hydroxyl, and His82 is associated with Asp33 in forming a catalytic diad. The focus of this work is to provide a global view of the mechanism, assess cooperation between various catalytic residues, and determine the origin of enzyme activation by the hydrophobic leaving group. To this end, we have investigated kinetic properties of Arg69, Asp33, and His82 mutants with phosphorothioate substrate analogues which feature leaving groups of varying hydrophobicity and pK_a. Our results indicate that interaction of the nonbridging pro-*S* oxygen atom of the phosphate group with Arg69 is strongly affected by Asp33, and to a smaller extent by His82. This result in conjunction with those obtained earlier can be rationalized in terms of a novel, dual-function triad comprised of Arg69, Asp33, and His82 residues. The function of this triad is to both activate the phosphate group toward the nucleophilic attack and to protonate the leaving group. In addition, Asp33 and His82 mutants displayed much smaller degrees of activation by the fatty acid-containing leaving group as compared to the wild-type (WT) enzyme, and the level of activation was significantly reduced for substrates featuring the leaving group with low pK_a values. These results strongly suggest that the assembly of the above three residues into the fully catalytically competent triad is controlled by the hydrophobic interactions of the enzyme with the substrate leaving group.

Phosphatidylinositol-specific phospholipase C (PI-PLC)[1] is a key effector of signal transduction in higher organisms (*1*). This enzyme is activated in response to binding of a hormone to an extracellular receptor and cleaves the P−O bond of phosphatidylinositol (PI, **1**) by a mechanism that involves the 2-hydroxyl group of inositol as an intramolecular nucleophile. In the past, we have determined that the mechanism of enzymes from mammalian tissues at the substrate level is analogous to those of the simpler bacterial enzymes (*2*−*4*). The bacterial enzymes differ from the mammalian proteins in that the intramolecular nucleophilic attack of the 2-hydroxyl group on the phosphorus atom (Scheme 1) to form inositol 1,2-cyclic phosphate (**2**, IcP) is much faster than the subsequent hydrolysis of IcP to inositol 1-phosphate (**3**, IP) (*5*, *54*), while the mammalian enzymes hydrolyze the cyclic phosphate prior to releasing it from the active site (*3*, *6*). Despite this difference, the more stable and smaller bacterial enzymes can be used as surrogate models of mammalian PI-PLC for studying chemistry that is underlying enzymatic activity.

Scheme 1

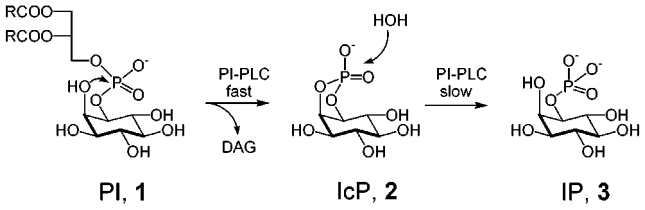

PI-PLC belongs to a broader class of phosphodiesterases that cleave β-hydroxyalkyl phosphoesters by the attack of an internal hydroxyl group on phosphorus to form a five-membered cyclic phosphate as an intermediate. This category of enzymes includes a large family of RNases among others (*7*); it is therefore not surprising that many analogies exist between mechanisms of RNases and PI-PLC, despite their vastly different structures. According to the most widely accepted mechanism of RNase A (*7*−*9*), the 2′-hydroxyl

† This work was supported in part by NIH Grants GM30327 (M.-D.T.) and GM57568 (K.S.B.). The NMR spectrometer was supported by NIH Grant S10 RR11283.

* To whom correspondence should be addressed. Telephone: (312) 996-4576. Fax: (312) 996-7107. E-mail: kbruzik@uic.edu.

‡ University of Illinois at Chicago.

§ Present address: Department of Chemistry, The Scripps Research Institute, 10550 N. Torrey Pines Rd., La Jolla, CA 92037.

|| The Ohio State University.

⊥ Present address: Department of Biochemistry, University of Wisconsin−Madison, Madison, WI 53706.

10.1021/bi002371y CCC: $20.00
Published on Web 04/14/2001

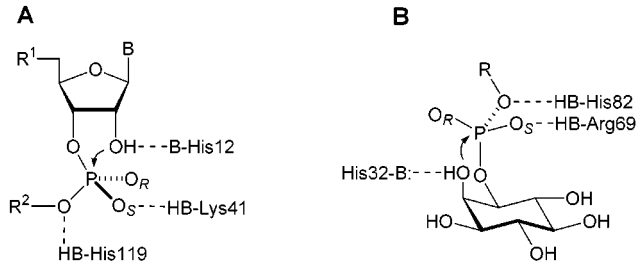

FIGURE 1: Comparison of major components of the active sites of PI-PLC and ribonuclease A.

group is deprotonated by the His12 residue (general base) and attacks the phosphorus atom (Figure 1A), while the 5′-oxygen is protonated by the imidazolium form of His119 (general acid). The function assigned to Lys41 is the subject of controversy (*10*), and ranges from forming a strong, low-barrier hydrogen bond to the nonbridging oxygen of the phosphate group (*8*, *11*) to electrostatic stabilization of the negative charge in the transition state (*12*).

The X-ray structure of *Bacillus cereus* PI-PLC (*13*, *14*) showed that, as for RNase A, its active site contains two histidines, His32 and His82, as well as Arg69 (Figure 1B). There is a major distinction between the two active sites, however, in that both histidines in PI-PLC are associated with aspartate residues to form His32−Asp274 and His82−Asp33 diads (*15*, *16*). In addition, the His32−Asp274 diad further interacts with the 2-hydroxyl group of inositol (*14*), to form a catalytic triad analogous to those found in serine proteases. The X-ray structure of the complex of PI-PLC with a partial substrate analogue, inositol (*13*, *14*, *17*), showed that Asp274 and His32, and His32 OH2, are within hydrogen bonding distances of 2.7 and 2.8 Å, respectively. In addition, the carboxyl function of Asp274 and the imidazole residue of His32 are coplanar (*14*), in optimal arrangement for charge relay within the triad. Furthermore, a low-field NMR signal observed in ^{1}H NMR spectra of PI-PLC suggested the existence of a low-barrier hydrogen bond between His32 and Asp274 (*18*). Thus, the structure and the catalytic function of the nucleophile-activating part of the active site seem well optimized for catalysis, both in the unliganded enzyme and in its complex with inositol. The subsequent studies by site-directed mutagenesis fully confirmed the functional significance of His32 and Asp274 as that of a complex general base (*15*).

In contrast, the available X-ray structures provide much less information about two other elements of mechanism: general acid catalysis and phosphate activation. These are also aspects of catalysis which are subject to perennial debate in the case of ribonucleases. Our previous SDM study indicated that His82 is involved in interactions with Asp33 to form a general acid diad (shown in Figure 10 of ref *15*), the function of which is to assist the leaving group by protonation or hydrogen bonding. This conclusion has been reached on the basis of kinetic evaluation of His82 and Asp33 mutants with substrates featuring low-pK_a leaving groups, such as *p*-nitrophenoxide (*15*) or mercaptide (*15*, *19*). In general, Asp33 and His82 mutants displayed much higher reactivity with these substrates than would have been predicted from the reactivity of these mutants with the normal substrate. These results are supported by the X-ray structure of the PI-PLC−inositol complex (*13*) which indicates hydrogen bonding interaction between His82 and Asp33. The relatively large distance between these residues (3.2 Å) and the perpendicular orientation of the carboxylate and imidazole groups indicate, however, that this diad is not in the optimal arrangement to perform the charge relay function.

Another major disparity between the RNase A and PI-PLC is in the mode of stabilization of the negative charge of the phosphate group. This is manifested by the large difference in the magnitude of kinetic effects of sulfur substitution for the nonbridging phosphate oxygens (k_O/k_S, thio effect) in substrates for both enzymes. For example, the RNase A-catalyzed cleavage of R_p- and S_p-diastereomers of 2′,3′-cyclic nucleoside phosphorothioate and 3′,5′-dinucleoside phosphorothioate showed a small thio effect ranging from 2 to 70 (*10*, *20*, *21*). In contrast, cleavage of phosphorothioate analogues of IcP (IcPs) and dipalmitoylphosphatidylinositol (DPPsI) by bacterial PI-PLC displayed an extremely high thio effect ($k_O/k_S = 1.6 \times 10^5$) (*19*, *22*). The facts that substitution of the pro-*S* oxygen with sulfur results in resistance to cleavage and that mutation of Arg69 to lysine reduces the S_p-thio effect by four orders (!) of magnitude (*22*) suggest that Arg69 is involved in interaction with the pro-*S* oxygen atom. The possibility that the interaction of Arg69 with the pro-*S* oxygen is quite feasible was confirmed by molecular modeling of the complex of PI-PLC with *O*-methyl inositol 1,2-cyclic phosphorane (pentacoordinated analogue of the TBP transition state) which showed that Arg69 is within 2.8 Å of the pro-*S* nonbridging oxygen of the phosphorane, while His82 is 3.7 Å away from the glycerol *sn*-3 oxygen (K. S. Bruzik and P.-G. Nyholm, unpublished results). The structural data acquired previously did not indicate any functional relationship between Arg69 and the general acid diad. Although the X-ray structure showed proximity of Arg69 and Asp33 (3.0 Å) (*14*), the functional significance of this interaction was unclear.

In the past, we have described structure−function studies (*15*, *16*, *19*, *22*−*24*) aimed at determining the catalytic roles of individual amino acid residues of the active site. The focus of this paper is to describe a global view of the catalytic site, and emphasize coordination of the roles of several catalytic functions into a single catalytic machinery. To achieve this goal, we have employed the concept of "matched substrate−enzyme mutagenesis". In this approach, we compare kinetic parameters of four pairs of reactants: (i) WT enzyme and natural substrate, (ii) mutant enzyme and natural

[1] Abbreviations: diC$_6$PC, 1,2-dihexanoyl-*sn*-glycero-3-phosphocholine; DIPEA, diisopropylethylamine; DOsPI, (2*R*)-1,2-dioctanoyloxypropanethio-3-(1-phospho-1*D*-*myo*-inositol); DOsPsI, (2*R*)-1,2-dioctanoyloxypropanethio-3-(1-thiophospho-1*D*-*myo*-inositol); DPPI, 1,2-dipalmitoyl-*sn*-glycero-3-(1-phospho-1*D*-*myo*-inositol); DPPsI, 1,2-dipalmitoyl-*sn*-glycero-3-(1-thiophospho-1*D*-*myo*-inositol); DPsPI, (2*R*)-1,2-dipalmitoyloxypropanethio-3-(1-phospho-1*D*-*myo*-inositol); DTP, 4, 4′-dithiobispyridine; ES-MS, electrospray mass spectrometry; Glu-1-P, glucose 1-phosphate; Gro-PI, *sn*-glycero-3-(1-phospho-1*D*-*myo*-inositol); Gro-sPI, (2*R*)-1,2-dihydroxypropanethio-3-(1-phospho-1*D*-*myo*-inositol); HDPC, hexadecylphosphorylcholine; HPAEC, high-pH anion exchange chromatography; IP, *myo*-inositol 1-phosphate; IcP, *myo*-inositol 1,2-cyclic phosphate; IcPs, *myo*-inositol 1,2-cyclic phosphorothioate; MOPS, morpholinepropanesulfonic acid; NPIPs, *p*-nitrophenyl 1*D*-*myo*-inositol phosphorothioate; PAD, pulsed amperometric detection; PI, phosphatidylinositol; PI-PLC, phosphatidylinositol-specific phospholipase C; SDC, sodium deoxycholate; SDM, site-directed mutagenesis; TBP, trigonal bipyramidal; UcP, uridine 2′,3′-cyclic phosphate; 3′-UMP, uridine 3′-phosphate; 3′,5′-UpA, uridyl(3′,5′)uridine; WT, wild type.

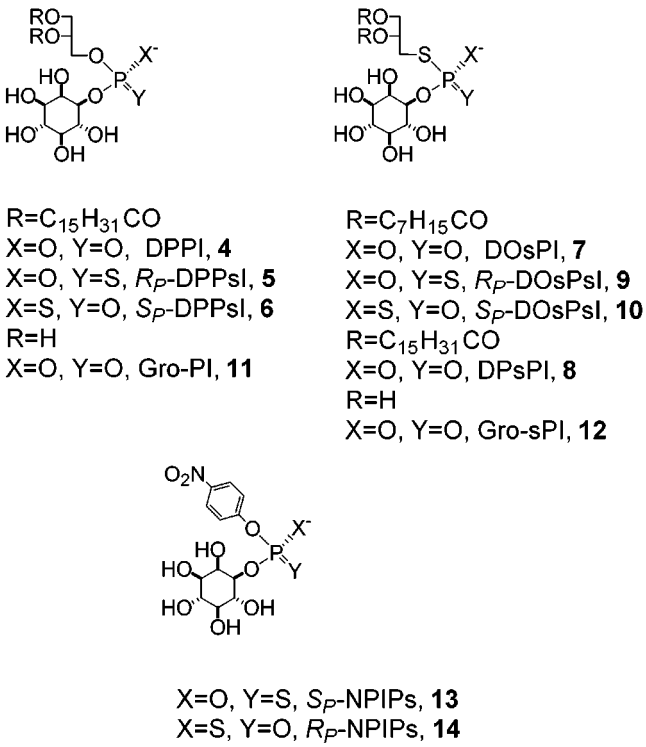

FIGURE 2: Structures of substrate analogues used in this work.

substrate, (iii) WT enzyme and substrate analogue, and (iv) mutant enzyme and substrate analogue. In the last pair, alteration at the specific substrate site is matched by mutation of a specific enzyme residue suspected of performing functional interaction with that substrate site. If the decreased catalytic rates in the cases of pairs ii and iii as compared to that of pair i are due to the removal of the same stabilizing factor, no further activity decrease should be observed in case iv. This methodology enables detailed description of the functional relationship between the substrate and enzyme residues and further refinement of the enzyme mechanism. To investigate interactions between the phosphate and active site residues, we have used the natural substrate DPPI (**4**, Figure 2), its phosphorothioate analogues (R_p)- and (S_p)-DPPsI (**5** and **6**, respectively), phosphorothiolate analogues DOsPI and DPsPI (**7** and **8**, respectively), and phosphorodithioate analogues (R_p)- and (S_p)-DOsPsI (**9** and **10**, respectively). Our results support strong cooperative effects between substrate and enzyme residues and in particular indicate involvement of a novel catalytic triad, including His82, Asp33, and Arg69, performing dual tasks of leaving group protonation and phosphate activation (*23*). In addition, we employed the same approach to study the effect of the full structure of the leaving group on the catalytic mechanism. In this case, we used substrate analogues devoid of hydrophobic chains and featuring leaving groups with varying pK_a values, such as *sn*-glycero-3-(1-phosphoinositol) (Gro-PI, **11**) 1,2-dihydroxypropanethio-3-(1-phospho-1*D*-*myo*-inositol) (Gro-sPI, **12**), and the corresponding *p*-nitrophenyl thiophosphoinositols, (S_p)-NPIPs (**13**) and (R_p)-NPIPs (**14**). The results obtained from the latter series of experiments present clear evidence that the assembly of the Arg, Asp, and His residues into the functional catalytic triad is affected by hydrophobic interactions of the enzyme with hydrocarbon chains of the substrate leaving group.

MATERIALS AND METHODS

Materials

DPPI and DPsPI were obtained analogously as described recently (*25*, *26*) starting from 2,3,4,5,6-pentakis(*O*-methoxymethylene)-*myo*-inositol (**15**; see the Supporting Information), and DPPsI was synthesized as reported previously (*3*). Natural PI was purified from soy bean phosphoinositide (Sigma) by chromatography on silica gel using a chloroform/methanol/water/ammonium hydroxide mixture (1.6:0.8:0.05:0.01, v/v) as the eluting solvent. NPIPs was synthesized as reported recently (*15*), and NPIP (*27*) was prepared by a slight modification of this procedure. Gro-PI (*28*) was obtained by deacylation of DPPI with methylamine in a methanol solution at room temperature over the course of 24 h. The fatty acid methylamide was removed by extraction of the aqueous solution of the reaction mixture with a methanol/chloroform mixture (4:6), and the aqueous phase was concentrated to give the pure product. Due to competing cyclization, DPsPI was deacylated into Gro-sPI using the lipase-catalyzed reaction (see the Supporting Information). Diisopropylethylamine (DIPEA), *O*-methyl phosphorodichloridite, 4,4′-dithiopyridine (DTP), and tetra-*n*-butylammonium periodate were from Aldrich. Esterase, MOPS, and Trizma base were from Sigma. All organic solvents were from Fisher, and were not further purified for chromatographic use. For their use as reaction media, solvents were dried over appropriate desiccants, stored in vacuum ampules prior to use, and transferred directly to reaction glassware by distillation under vacuum. WT PI-PLC and its mutants were expressed and purified as reported previously (*15*, *22*). All NMR spectra were recorded with a Bruker DPX-300 spectrometer. The ES-MS spectra were obtained with a Micromass Quatro II tandem mass spectrometer.

Assays of PI-PLC Activity

^{31}P NMR Assay. All kinetic runs were performed in 50 mM MOPS buffer (sodium salt) at pH 7.0 in the presence of 5 mM Na-EDTA and 10% D_2O. The substrate concentration was 10 mM, and the detergent concentration was 40 mM, except for sodium deoxycholate which was used at a concentration of 20 mM. Glucose 1-phosphate (Glu-1-P) was used as an internal standard for quantitation. Each sample was prepared in the following manner. The appropriate amounts of the substrate and detergent in an Eppendorf tube were dispersed by vortexing in the buffer solution (200 μL) containing 100 mM MOPS, 10 mM EDTA (pH 7.0), H_2O (156 μL), D_2O (40 μL), and a glucose 1-phosphate solution (0.56 M, 4 μL) and quantitatively transferred into a 5 mm NMR tube. Prior to the assay, the sample was sonicated in the ultrasonic bath to achieve optical transparency. Kinetic runs were performed at 25 °C, and spectra were recorded at 121.5 MHz with a Bruker DPX-300 spectrometer. Acquisition parameters were as follows: pulse width, 4.2 μs; sweep width, 18 kHz; acquisition time, 0.50 s; relaxation delay, 0.50 s; time domain, 18K; size, 32K; and digital resolution, 0.55 Hz. For all kinetic runs, a control spectrum was obtained ($t = 0$ min) prior to adding the enzyme. The reaction was initiated by adding 50 ng to 0.5 mg of PI-PLC depending on enzyme activity. The volume of enzyme solution that was added varied from 0.25 to 10% of the sample volume (from

1 to 40 μL). The enzyme solutions were freshly prepared by dissolving the solid enzyme in distilled water. The concentration of the enzyme was determined spectrophotometrically (ϵ = 18 300 M^{-1} cm^{-1} at 280 nm). The amount of enzyme used for reaction was sufficient to achieve rates of about 0.05 μmol/min (1.25% conversion/min). Reactions were typically followed for about 1 h; however, reactions with a V_{max} of $<5 \times 10^{-3}$ μmol min^{-1} mg^{-1} were followed for a period of 4−14 days. The rate of substrate cleavage was calculated by comparing the integral intensity of IcP, or the sum of IcP and IP, with that of the internal standard Glu-1-P. The initial velocity was obtained by fitting the linear portion of the kinetic curve with Cricket Graph 1.3.2 software.

Spectrophotometric Assay of PI-PLC with Gro-sPI. The spectrophotometric method used here is a modification of the procedure reported by Hendrickson and co-workers (*28*). Upon reaction with PI-PLC, **12** was converted into IcP and 1,2-dihydroxy-3-mercaptopropane. The latter product reacted with 4,4′-dithiopyridine (DTP) to release 4-mercaptopyridine, allowing spectrophotometric determination of the amount of product formed, by measuring the UV absorbance at 324 nm. An aliquot of the concentrated stock solution of **12** (100 mM) in water was diluted with buffer [50 mM Na-MOPS and 0.5 mM Na-EDTA (pH 7.0)] to obtain the desired substrate concentration (0.5−6 mM) prior to the assay. The diluted substrate solution (970 μL) was placed in a semimicro UV cuvette, and the solution of DTP in ethanol (20 μL, 50 mM) was added. The contents of the cuvette were stirred and equilibrated for 5 min at 25 °C. A background reaction rate was recorded for 2 min against the MOPS buffer as a reference solution. PI-PLC (10 μL, 13.9 μg) was added, and the absorbance at 324 nm was recorded for 5−10 min. The molar extinction coefficient of 4-mercaptopyridine (ϵ = 19 800 M^{-1} cm^{-1}) was used to calculate the initial reaction rates. The Lineweaver−Burke treatment of data gave a linear plot of 1/*V* versus 1/[Gro-sPI].

*HPAEC Assay of PI-PLC with sn-Glycero-3-(1-phospho-1D-myo-inositol) (Gro-PI, **11**).* High-pH anion exchange chromatography (HPAEC) coupled with pulsed amperometric detection (Dionex, PAD-2) was employed to quantitate IcP and IP. The Carbopack PA1 column (Dionex, 4.6 mm × 250 mm) was eluted with a sodium acetate gradient (from 40 to 200 mM over the course of 15 min) in isocratic 100 mM sodium hydroxide (1 mL/min flow rate). Elutions were monitored with the detector sensitivity set at 1 μA, and the ionization potentials set as follows: E_1 = 0.05 V, E_2 = 0.6 V, and E_3 = −0.6 V. Glucose 1-phosphate was used as an internal standard to ensure high accuracy of measurement of IcP and IP concentrations. Quantitation of IcP and IP, both products of the enzymatic reaction of Gro-PI with PI-PLC, was performed by obtaining calibration curves for each compound (see the Supporting Information). Five duplicate samples of IcP and IP with concentrations of 0.2, 0.4, 0.6, 0.8, and 1 mM were prepared, each containing 0.2 mM Glu-1-P. The samples were chromatographed, and signals at 4.5 (Gro-PI), 8.7 (IcP), 11.7 (IP), and 13.2 min (Glu-1-P) were integrated. The plots of the IcP/Glu-1-P and IP/Glu-1-P area ratios versus the concentration of IcP and IP were linear and had slopes of 1.56 and 0.6, respectively. These slopes were used to calculate quantities of IcP and IP from HPAEC chromatograms.

An aliquot of the concentrated stock solution of Gro-PI (100 mM) in buffer [50 mM Na-MOPS and 0.5 mM Na-EDTA (pH 7.0)] was diluted with the same buffer to obtain a desired concentration of Gro-PI (1−50 mM). Into this sample was added the Glu-1-P solution (2 μL, 10 mM), and the volume was adjusted to 95 μL with buffer, followed by addition of PI-PLC (5 μL containing 4.65 μg of WT, 25 μg of D33N, or 100 μg of D33A). The reaction mixture was stirred for 2 min, and an aliquot (1−5 μL) was injected onto the HPAEC column. The time course of the sum of concentrations ([IcP] + [IP]) was plotted for each concentration of Gro-PI; the initial slopes were calculated, and the V_{max} and K_m values were determined from the double-reciprocal plot of 1/*V* versus 1/[Gro-PI].

RESULTS AND DISCUSSION

Chemical versus Physical Rate-Limiting Step. Before evaluation of the functional contribution of an enzyme or substrate residue to catalysis, it is imperative to determine whether the chemical step is a rate-limiting one. If a physical event is a rate-limiting factor, changes in free energies of activation due to substrate and/or enzyme modifications are not reflected in the overall catalytic rates (*29*, *30*), and false conclusions would be drawn about functional substrate−enzyme interactions. To address this problem, we have examined the kinetics of reactions of WT and mutant enzymes with several substrates dispersed in various detergents. With DPPI as the substrate, the highest rates of cleavage were obtained with diC_6PC and SDC detergents, while the long, single-chain detergent, HDPC, produced ∼30-fold lower rates (Table 1). The difference between the detergents almost completely disappeared in reactions of DPPI with "slow mutants" (such as D33A and D33N), and those of WT with "slow substrates" [such as DOsPI, DPsPI, and (R_p)-DPPsI (Table 2)].

The most plausible explanation of the above results is that with HDPC/DPPI micelles as the substrate, a physical event, e.g., lateral diffusion of a substrate molecule on the micelle surface or lipid exchange between micelles, rather than P−O bond formation and/or cleavage, is a rate-determining step. This conclusion is supported by the observation that in ^{31}P NMR spectra of PI/HDPC dispersions, the line width of the substrate NMR signal is broader than those of PI/SDC or PI/diC_6PC dispersions (data not shown), suggesting slow molecular tumbling in the former. With HDPC as a detergent, the chemical step becomes rate-limiting when catalysis is made less efficient, such as in the cases of relatively sluggish mutants or less reactive substrates (with a V_{max} of less than ∼50 μmol mg^{-1} min^{-1}). This is because it is highly unlikely that single-residue mutation of the enzyme or minor alteration of the substrate structure (such as O → S replacement) would in any significant way affect the rates of these diffusional processes. Hence, the chemical step should be rate-limiting for the (R_p)-DPPsI−WT pair and other less reactive enzyme−substrate pairs, the activities of which are not responsive to the detergent change. It is, however, possible that the highest rates observed in this work could be capped by a physical step. The fact that the same highest activity (∼2000 μmol mg^{-1} min^{-1}) is observed with two structurally unrelated detergents (SDC and diC_6PC) suggests, however, that such physical step limitation, if it indeed exists, is unrelated to lipid−water interface phenomena.

Table 1: Activities of PI-PLC Mutants toward DPPI and (R_p)- and (S_p)-DPPsI[a]

enzyme−detergent	DPPI	(R_p)-DPPsI	(S_p)-DPPsI	thio effect k_O/k_{R_p}	thio effect k_O/k_{S_p}	stereoselectivity k_R/k_S
WT−diC$_6$PC	$(2.0 \pm 0.18) \times 10^3$	53 ± 3.4	$(6.5 \pm 0.4) \times 10^{-3}$	37 ± 7	$(3.1 \pm 0.5) \times 10^5$	$(8.2 \pm 1) \times 10^3$
WT−SDC	$(1.1 \pm 0.13) \times 10^3$ [b]	29 ± 3	$(1 \pm 0.1) \times 10^{-3}$	38 ± 13	$(1.1 \pm 0.3) \times 10^6$	$(29.6 \pm 6) \times 10^3$
WT−HDPC	60 ± 0.2	11 ± 1	$(4.8 \pm 0.5) \times 10^{-3}$	5.5 ± 0.5	$(1.3 \pm 0.1) \times 10^4$	$(23.5 \pm 4.5) \times 10^2$
D33E−diC$_6$PC	1.1 ± 0.04	$(6.6 \pm 0.8) \times 10^{-3}$	$(1.2 \pm 0.2) \times 10^{-4}$	167 ± 30	$(9.2 \pm 2.2) \times 10^3$	58 ± 16
D33N−diC$_6$PC	11 ± 0.9	2.0 ± 0.1	$(7 \pm 0.6) \times 10^{-2}$	6.0 ± 0.3	157 ± 29	29 ± 4
D33N−HDPC	8.2 ± 0.4	1.0 ± 0.1	0.17 ± 0.04	8.2 ± 1.6	48 ± 18	6 ± 2
D33A−diC$_6$PC	4.6 ± 0.1	$(4.7 \pm 0.3) \times 10^{-2}$	$(9 \pm 1) \times 10^{-3}$	98 ± 9	511 ± 77	5 ± 1
D33A−HDPC	3.6 ± 0.2	$(1.2 \pm 0.2) \times 10^{-2}$	$(6 \pm 0.8) \times 10^{-3}$	300 ± 80	600 ± 130	2 ± 0.5
H82A−SDC[b]	$(9.2 \pm 0.2) \times 10^{-3}$					
D67A−diC$_6$PC	$(2.2 \pm 0.1) \times 10^3$	110 ± 10	$(6 \pm 0.7) \times 10^{-3}$	20 ± 3	$(3.7 \pm 0.37) \times 10^5$	$(18.8 \pm 3.8) \times 10^3$
D198N−diC$_6$PC[b]	6.9 ± 0.3					

[a] All activities are expressed in micromoles per minute per milligram. DPPsI was a 57/43 mixture of the S_p- and R_p-diastereomers. The reaction rates were determined by ^{31}P NMR. [b] Obtained for PI from soybean.

Table 2: Activities of PI-PLC Mutants toward DOsPI and DOsPsI[a]

enzyme−detergent	DOsPI	k_O/k_S	(R_p)-DOsPsI	(S_p)-DOsPsI	k_{R_p}/k_{S_p}
WT−diC$_6$PC	58 ± 5	34 ± 7	15 ± 1	0.67 ± 0.07	22 ± 5
WT−HDPC	64 ± 6	0.94 ± 0.01			
WT−SDC	53 ± 5	21 ± 5			
D33N−diC$_6$PC	0.68 ± 0.04	16.3 ± 2.3	0.84 ± 0.06	0.10 ± 0.01	8 ± 2
D33N−HDPC	0.74 ± 0.06	11.1 ± 1.4			
D33A−diC$_6$PC	49 ± 3	0.094 ± 0.008	3.0 ± 0.02	0.10 ± 0.01	30 ± 4
D33A−HDPC	62 ± 4	0.58 ± 0.07			
H82A−diC$_6$PC			$(5 \pm 0.3) \times 10^{-3}$	$(0.6 \pm 0.1) \times 10^{-3}$	8 ± 2
R69A−diC$_6$PC	1.57×10^{-3}	2.7	$(2.1 \pm 0.1) \times 10^{-4}$	$(0.9 \pm 0.2) \times 10^{-4}$	2 ± 1
D198N−diC$_6$PC	0.88 ± 0.07	7.8 ± 1			

[a] All activities are expressed in micromoles per minute per milligram. The activities were determined by ^{31}P NMR.

Effect of Sulfur Substitution on Substrate Binding Properties. Since much of the kinetic data reported in this work were obtained for phosphorothioate analogues of PI, it is essential to assess the effect of sulfur substitution on substrate binding properties. Furthermore, since many kinetic data were obtained using the mixture of R_p- and S_p-diastereomers of DPPsI as a substrate, it is also important to estimate the magnitude of the inhibitory effect of one diastereomer on reaction rates of another one. Thus, with DPsPI as the assay substrate (K_m = 0.26 mM), the K_i values for the R_p- and S_p-isomers were 2.1 and 0.56 mM, respectively (see the inhibition data in the Supporting Information). In addition, the V_{max} value for the cleavage of DPPI in the presence of equal concentrations of both (R_p)- and (S_p)-DPPsI was 612 μmol mg^{-1} min^{-1}, ~3-fold lower than that for DPPI alone. In agreement with the above, the V_{max} values for the cleavage of individual diastereomers were as follows: 206 μmol mg^{-1} min^{-1} for (R_p)-DPPsI, ~4-fold higher than for the R_p/S_p mixture (1:1); and 0.014 μmol mg^{-1} min^{-1} for (S_p)-DPPsI, 2-fold higher than for the mixture. Given that the K_m value for DPPI is ~1 mM (*31*), these results indicate that introduction of sulfur into the nonbridging position of PI does not significantly affect ground-state binding properties of the substrate. On the other hand, introduction of sulfur into the bridging position lowers the K_m value several-fold (*15*, *25*).

Effects of Sulfur Substitution on Enzyme Activity: Nonbridging Thio Effects. Phosphate activation toward nucleophilic attack can be realized by hydrogen bonding or protonation of either the pro-*R*, pro-*S*, or both phosphoryl oxygen atoms. Substituting sulfur for an oxygen atom acting as a Brønsted base strongly diminishes such interactions, resulting in significantly lower rates for sulfur-containing substrates. The activity ratios between the oxygen- and sulfur-containing substrates (thio effect, k_O/k_S) is related to the strength of such protonic interactions, whereas the position, the substitution of which alters the activity to a greater extent, indicates which of the two pro-*R* or pro-*S* oxygens of the phosphate group is the interaction site. In the past, we have studied the effect of nonbridging sulfur on activities of the WT and Arg69 mutants (*19*, *22*). In this work, we examined the effect of mutations at positions which are not directly involved in interactions with phosphoryl oxygens, such as Asp33 and His82. Activities of PI-PLC and its mutants toward DPPI, (R_p)-DPPsI, and (S_p)-DPPsI, the stereospecific thio effects (k_O/k_{R_p} and k_O/k_{S_p}), and the R_p/S_p stereoselectivity (k_{R_p}/k_{S_p}) are summarized in Table 1.

For WT PI-PLC and substrates presented as diC$_6$PC and SDC dispersions, replacement of the pro-*R* oxygen in DPPI with sulfur (k_O/k_{R_p} thio effect) resulted in the 30−50-fold decreases in activity, somewhat larger than those that we reported previously (Table 1) (*19*, *22*). In contrast, the replacement of the pro-*S* oxygen with sulfur (k_O/k_{S_p} thio effect) resulted in extremely large reductions in activity on the order of 10^5-10^6-fold. Consequently, the R_p/S_p stereoselectivity was also very high, ~8000−30000. Since we regarded Asp33 as an intimate part of the general acid diad (*15*, *16*), it was surprising to note that any mutation of this residue resulted in a significant decrease in the magnitude of the thio effect and stereoselectivity. Thus, the D33N mutant exhibited a 6-fold reduction in k_O/k_{R_p} and a 2000-fold reduction in k_O/k_{S_p}, as compared to the values for the WT in diC$_6$PC micelles. Interestingly, the low value of k_O/k_{S_p} is due to both a decrease in k_O and an increase in k_{S_p}. Thus, with (S_p)-DPPsI as a substrate, the D33N mutant was 11-fold more active than the WT enzyme in diC$_6$PC micelles. The behavior of the D33A mutant was similar to that of

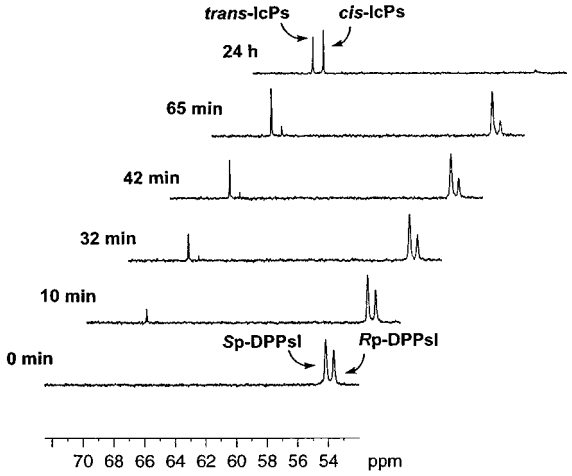

FIGURE 3: Time course of the cleavage of (R_p/S_p)-DPPsI with the D33A mutant as monitored by ^{31}P NMR. Reaction conditions: 10 mM (R_p/S_p)-DPPsI, 20 mM SDC in Na-MOPS buffer (20 mM, pH 7.0), 53 μg of the D33A mutant, temperature of 25 °C.

D33N: a 3-fold increase in k_O/k_{R_p} and a 600-fold decrease in k_O/k_{S_p} as compared to those of the WT. As a result, the ratios of the V_{max} values for the cleavage of the R_p- and S_p-diastereomers (R_p/S_p stereoselectivities) by D33A and D33N mutants were also very small, ranging from 2 to 58. A clear illustration of a low discrimination factor between the two diastereoisomers by the D33A mutant is shown as the time course of the cleavage of the (R_p/S_p)-DPPsI mixture (Figure 3), where simultaneous formation of both *trans*- and *cis*-isomers of IcPs is apparent. The data presented above implicate strong functional interaction between Arg69 and Asp33 residues. Since we have previously demonstrated functional interaction of the same Asp33 with His82, these results collectively indicate the existence of a novel catalytic assembly involving Arg69, Asp33, and His82.

Mechanistic Interpretation of Thio Effects in PI-PLC. There are two types of kinetic effects of O → S structure modification, depending on the modification site. (i) With the sulfur atom located in the nonscissile bond (nonbridging position), the thio effect could be a direct consequence of decreased hydrogen bonding stabilization of the transition state. The other possible effect of sulfur presence could be due to an increased steric size of a phosphorothioate group as compared to phosphate (*32*). The resulting unfavorable steric interactions in the transition state could affect alignment and cooperation between essential catalytic residues of the active site (*32*). The latter possibility, although it cannot be ruled out completely in the case of PI-PLC, appears to be less likely. This is because as we have shown here, and has been reported by others (*33*), the O → S modification of PI at the nonbridging positions has a relatively minor effect on ground-state binding to PI-PLC. Furthermore, variation of the side chain length at position 69 only moderately influences the magnitude of the thio effect, and has virtually no impact on R_p/S_p stereoselectivity (*34*). Potential complications resulting from the increased steric size of phosphorothioate as compared to phosphate, as well as from the somewhat different electron distribution in these two types of substrates (*35*, *36*), are alleviated by the fact that many conclusions from this work are based on the comparison of the kinetic properties of two phosphorothioate diastereomers, where the steric size and electronic structures are the same.

In reactions of phosphodiesters not involving protic acid catalysis, the nonbridging thio effect is usually very small (*37*). For example, imidazole-catalyzed cleavage of *p*-nitrophenyl inositol phosphate (NPIP) and the corresponding phosphorothioates, (R_p)- and (S_p)-NPIPs, occurs with the same rate constant (*38*), and the thio effect for specific base-catalyzed cleavage of uridine 2′,3′-cyclic phosphorothioate (UcPs) is only 6 (*39*). In contrast, the thio effect for the specific acid-catalyzed cleavage of 2′,3′-UcPs is ∼200 (*39*). In this work, we have determined the rate constants of both specific acid- and base-catalyzed cleavage of IcP and IcPs as our reference points. The obtained rate constants of IcP and IcPs are close to those of UcP and UcPs (*39*) and are as follows: $k = 1.5 \times 10^{-3}$ s^{-1} for 0.15 M $HClO_4$ and IcP, $k = 5 \times 10^{-6}$ s^{-1} for 0.15 M $HClO_4$ and IcPs, $k = 5.5 \times 10^{-4}$ s^{-1} for 0.25 M KOH and IcP, and $k = 1.4 \times 10^{-4}$ s^{-1} for 0.25 M KOH and IcPs. Hence, the magnitude of the thio effect for acid-catalyzed cleavage of IcP is 300, and that for the hydroxide-catalyzed cleavage is only 4. It is worth mentioning that chemical acid-catalyzed hydrolysis occurs probably without much distinction between protonation at the pro-*R* and pro-*S* sites; therefore, one could expect a much greater nonbridging thio effect if protonation was stereospecific.

(ii) With the sulfur located in the scissile bond (bridging position), the magnitude of the thio effect depends on the balance of two mutually compensating factors. A loss of most of hydrogen bonding stabilization of the leaving group upon sulfur substitution reduces the catalytic rate, whereas the decrease in the pK_a of the leaving group (pK_a = 9.5 for mercaptide and pK_a = 14.5 for alkoxide) increases the inherent chemical reactivity of the substrate. As a reference point, we studied the effect of sulfur substitution of the bridging oxygen in *sn*-3-glycerophosphoinositol (Gro-PI) on chemical reactivity under the base-catalyzed condition. The reactivity of Gro-PI in 0.25 M KOH expressed as a sum of the second-order rate constants for formation of IcP and IP was 6.5×10^{-5} M^{-1} s^{-1}, and that of Gro-sPI was 3.4×10^{-2} M^{-1} s^{-1}. This ∼500-fold increase in reactivity should be considered as an upper limit, since in the enzyme-catalyzed reactions the degree of charge development on the leaving group is smaller than that in the chemical reaction (*15*, *40*). The net bridging thio effect would thus depend on the balance of the energy of hydrogen bonding to the natural oxygen-containing leaving group and energy of stabilization of the negative charge developing in the transition state by the more stable mercaptide leaving group in the substrate analogue. In general, WT enzymes should produce large nonbridging thio effects (≫1), whereas enzyme mutants deficient in leaving group stabilization should display small (∼1) or inverse bridging thio effects (<1).

The results in Table 1 show that the stereospecific thio effects in the WT enzyme upon substitution of the pro-*S* oxygen (k_O/k_S) are on the order of 10^5−10^6-fold, corresponding to the loss of 7−8 kcal/mol in the overall stabilization energy, whereas substitution at the pro-*R* site is associated with only a modest decrease in activity. The results of this and the accompanying work (*34*) indicate that this loss of stabilizing energy due to sulfur substitution results from alteration of two types of interactions: (i) hydrogen bonding or proton transfer to nonbridging and bridging oxygens and (ii) bringing the phosphate group into proximity with the

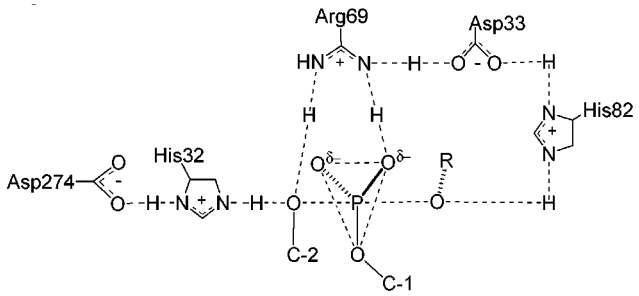

FIGURE 4: Mechanism of PI-PLC proposed on the basis of this study, showing the function of the Arg69−Asp33−His82 triad. The interaction between Arg69 and the 2-OH of inositol is supported by the results reported in the following paper in this issue (*34*).

attacking hydroxyl group, i.e., formation of the near-attack conformation. The latter depends on simultaneous interactions of Arg69 with the 2-OH group and the pro-*S* phosphoryl oxygen, and is most likely affected by sulfur modification (*34*). The most important result of this work is the finding that the *magnitude of the nonbridging thio effect is greatly reduced in both D33 mutants*. This result has far-reaching implications. First, the catalytic role of Asp33 is not limited to association with the His82 general acid, as we envisioned earlier (*15*). It is clear that interaction of Asp33 with Arg69 is also very important for catalysis. Hence, a part of the decrease in activity for Asp33 mutants results from the loss of the influence of Asp33 on the acid−base property and/or orientation of the Arg69 side chain.

Catalytic Mechanism Involving the Arg69−Asp33−His82 Triad. Since we have previously established the complex nature of the general acid as consisting of Asp33 and His82 residues (*15*), and we now show the importance of Asp33−Arg69 interactions, these results indicate collectively that the functions of all three residues are inseparable. We propose that the three residues form a catalytic triad involved in both phosphate stabilization and leaving group protonation (Figure 4). The details of the communication within the triad and with the phosphate group, however, remain unclear, particularly regarding the specific nature of the interaction between Arg69 and the phosphate. In our view, the data presented here are most consistent with a dual general acid mechanism where the two general acids, Arg69 and His82, are tracking the progress of charge buildup on the nonbridging and leaving group oxygens, making hydrogen bonding contacts, or transferring protons as needed. In the initial phase of the reaction, the approach of the negatively charged inositol 2-oxygen toward phosphorus is facilitated by hydrogen bonding to the nonbridging oxygen by Arg69, whereas in the late stage of the reaction, the opposite would be beneficial, since the buildup of negative charge on the nonbridging oxygen would help repel the negative charge of the leaving group. This could be accomplished by the movement of the arginine proton away from the nonbridging oxygen with simultaneous movement of the imidazolium proton toward the bridging oxygen, to an extent depending on the position of the reactive complex on the reaction coordinate. Another potential function of the triad is to assist and coordinate formation of the reactive conformation of the substrate (near-attack conformation) (*41*). Such a conformation is characterized by the proximity of the 2-OH to phosphorus, the antiparallel orientation of the scissile P−O bond versus the attacking nucleophile, and the orientation

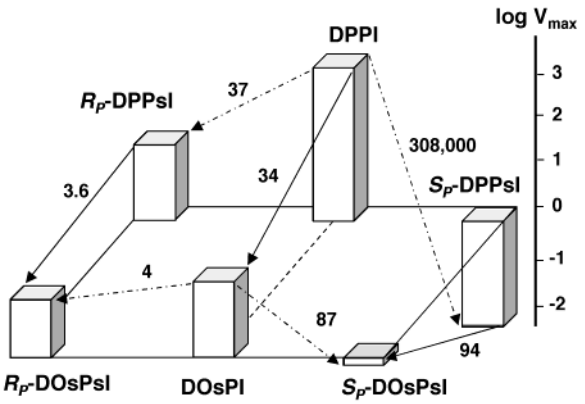

FIGURE 5: Diagrammatic representation of activities of WP PI-PLC with phosphorothioate and phosphorodithioate analogues of PI.

of the lone electron pair on the leaving group oxygen, consistent with its protonation by the His82 general acid.

To the best of our knowledge, this is the first observation of the bidentate catalytic triad performing a dual catalytic task. Other known triads such as the Ser−His−Asp triad of serine proteases (*42*) or the Cys−His−Asp(Asn) triad found in thiol proteases (*43*) are monodentate as they make only a single contact with the substrate molecule. The more recently identified triads include the Asp−His−Asp triad of epoxide hydrolase (*44*) and the Ser−His−His triad of CMV protease (*45*). In all these assemblies, the substrate-proximal residue such as Ser, Cys, or Asp serves as a nucleophile to form a reactive intermediate; the internal His functions as a general base activating the serine hydroxyl or water molecule, and the distal Asp (Glu) is the general base modifying the pK_a and/or tautomeric state of the His residue, and also acts as an orientation device for the imidazole residue. The Arg−Asp−His triad reported here is distinct from all those listed above in that it contains general acids at both flanks and makes double contact with the substrate molecule.

Interdependence of Nonbridging and Bridging Thio Effects: Phosphorodithioate Substrates. The function of the new Arg−Asp−His catalytic assembly is to make simultaneous stabilizing contacts with both bridging and nonbridging oxygens in the trigonal bipyramidal transition state. If these three residues indeed act cooperatively as proposed, alteration of interactions at the nonbridging oxygen site should affect those at the bridging site, and vice versa. To probe this possibility, we have studied the kinetic behavior of phosphorodithioate analogues in which sulfur replaces both the bridging and nonbridging oxygens (DOsPsI), and compared the obtained data with those obtained for phosphoromonothioates (DPPsI and DOsPI). In stark contrast to the extremely high R_p/S_p stereoselectivity displayed by the WT enzyme with phosphorothioate DPPsI isomers, the discrimination between R_p- and S_p-isomers of DOsPsI was reduced to only 22 upon introduction of a second sulfur atom into the bridging position, such as in phosphorodithioate, DOsPsI isomers (Table 2).

The effects of introducing the second sulfur atom are also diagrammatically shown in Figures 5 and 6. Thus, introduction of the first sulfur into the pro-*R* position or bridging position of DPPI results in an ∼37- and ∼34-fold decrease in activity, respectively (Figure 5). Introduction of the second sulfur atom into either the pro-*R* position of DOsPI or the

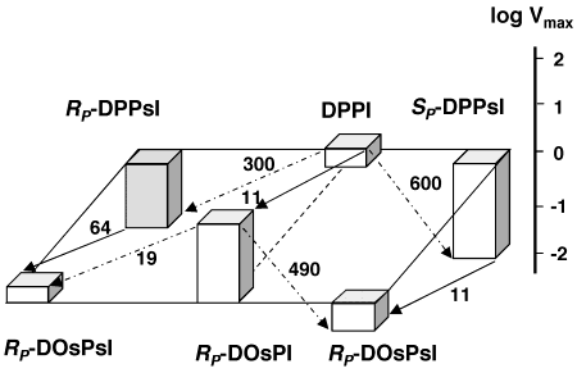

FIGURE 6: Relative activities of the D33A mutant with phosphorothioate and phosphorodithioate analogues of PI.

bridging position of (R_p)-DPPsI follows the same trend, although its effect is only 4-fold. This behavior is in great contrast to introducing sulfur into the pro-*S* position, where the first nonbridging sulfur reduces the activity more than 10^5-fold, whereas *introduction of the second sulfur into the bridge position of (S_p)-DPPsI actually increases the activity ~100-fold*. These results are interpreted as an indication that the removal of the nonbridging interactions [such as in (S_p)-DPPsI] also removes the bridging interactions [as manifested by the greater chemical reactivity of (S_p)-DOsPsI]. Likewise, the removal of the bridging interaction (such as in DOsPI) causes a significant reduction in the extent of nonbridging interactions [manifested by a small nonbridging thio effect for (S_p)-DOsPsI; $k_O/k_{S_p} = 87$]. In conclusion, the status of one interaction determines the strength of another, and hence, the transition state consists of substrate and enzyme groups which are closely communicating their status to both substrate and enzyme environments. Consistently, *a single break in the communication chain, such as in the D33A mutant, causes the bridging and nonbridging events to become unrelated* (Figure 6). Thus, for the D33A mutant, introduction of the nonbridging sulfur always results in a similar small reduction in activity (regardless of whether it goes to the pro-*S* or pro-*R* position, and whether it is the first or second sulfur). In contrast, introduction of the bridging sulfur always results in increased activity [regardless of whether it is introduced to DPPI or (S_p)- or (R_p)-DPPsI]. The observation of interdependence between bridging and nonbridging thio effects is complementary to the communication between Arg69 and His82. Showing it both ways diminishes the possibility that the communication between R69 and H82 is caused by structural effects in the mutants.

Interdependence of Nonbridging and Bridging Interactions: Substrates Featuring a Low-pK_a Leaving Group. In the previous section, we demonstrated the cooperativity between bridging and nonbridging interactions by inserting sulfur in place of the bridging oxygen and observing a significant decrease in the strength of nonbridging interactions. Similar, albeit smaller, effects should be observed for substrates where diminished bridging interactions are due to the lower pK_a value of the leaving group oxygen. It has been shown previously that aryl esters require less protonation and/or hydrogen bonding assistance from the general acid to their aryloxy leaving group (*9*). Weaker interactions to bridging oxygen should translate into weaker nonbridging interactions and result in lower R_p/S_p stereoselectivities for aryl esters than for alkyl esters. To test this hypothesis, we

Table 3: Activities of PI-PLC Mutants toward NPIPs Diastereomers[a,b]

	(R_p)-NPIPs	(S_p)-NPIPs	k_{S_p}/k_{R_p}
WT	0.045 ± 0.05	44 ± 5	978 ± 220
D33N	0.6 ± 0.05	4.8 ± 0.3	8.1 ± 1.2
D33A	0.2 ± 0.02	1.6 ± 0.1	8.1 ± 1.2
H82A	$(3.7 \pm 0.4) \times 10^{-3}$	0.6 ± 0.05	162 ± 30
R69A[c]	$(0.6 \pm 0.1) \times 10^{-4}$	$(3.7 \pm 0.2) \times 10^{-4}$	6 ± 2
D198N	$(2.5 \pm 0.3) \times 10^{-5}$	0.013 ± 0.01	520 ± 120

[a] The reaction rates were determined by ^{31}P NMR. All activities are expressed in micromoles per minute per milligram. [b] The assays were performed at subsaturating concentrations of NPIPs: 7.5 mM S_p-isomer and 5.75 mM R_p-isomer. [c] The activity of the R69A mutant with PI was 4.21×10^{-3} μmol min^{-1} mg^{-1} (*25*).

determined the k_{S_p}/k_{R_p} ratios for WT and mutant PI-PLCs toward the diastereomers of *p*-nitrophenyl inositol phosphorothioate [(S_p)- and (R_p)-NPIPs, **13** and **14**, respectively] and compared the results with the analogous data for the mixture of DPPsI isomers (Table 3). Please note that due to the reversal of ligand precedence around phosphorus in NPIPs, the S_p-isomer of NPIPs actually corresponds to the R_p-isomer of DPPsI. As predicted, the WT PI-PLC displayed ~10-fold reduced stereoselectivity with isomers of NPIPs as compared to DPPsI, mainly as a result of the increased reactivity of the nonpreferred isomer, (R_p)-NPIPs. Consistent with cooperativity of bridging and nonbridging effects, the H82A mutant exhibited a further 6-fold reduction in stereoselectivity. Like the behavior of D33 mutants with DPPsI diastereomers, a large reduction in stereoselectivity was observed with both of these mutants, due to the lower reactivity of (S_p)-NPIPs and the increased reactivity of (R_p)-NPIPs, as compared to the WT enzyme; however, no significant change was observed for the D198N mutant despite its low activity (crystal structure shows that D198 could not interact with the phosphate group).

Effect of Leaving Group Structure on Catalytic Functions of Asp33 and His82. PI-PLC activity is strongly affected by the presence of fatty acid chains in the substrate leaving group, with a large decrease in V_{max} and an increase in K_m upon removal of hydrophobic functions (*46*, *47*). Thus, nonhydrophobic substrate IcP displays a V_{max} of 22 μmol mg^{-1} min^{-1} and a K_m of 80 mM (*47*), and *p*-nitrophenyl inositol phosphate (**11**) has a V_{max} of 650 μmol mg^{-1} min^{-1} and a K_m of 5 mM (*27*). The assessment of the degree of impairment of catalytic efficiency due to the absence of hydrophobic chains in these two substrates is difficult, since the intrinsic reactivity of IcP, as compared to that of PI, is increased by the ring strain (*28*), and that of NPIP is increased due to the low pK_a of the leaving group.

To estimate the effects of the leaving group pK_a and the presence of hydrophobic chains on substrate reactivity, we have tested four substrates: DPPI (high-pK_a leaving group, hydrophobic), DOsPI (low pK_a, hydrophobic), *sn*-glycero-3-(1-phospho-1*D*-*myo*-inositol) (Gro-PI, **11**, Figure 2, high pK_a, nonhydrophobic), and (2*R*)-1,2-dihydroxypropane-3-(1-thiophospho-1*D*-*myo*-inositol) (Gro-sPI, **12**, low pK_a, nonhydrophobic). Within this series of substrates, a change in hydrophobicity is achieved without a significant change in pK_a (diacyl glycerol vs glycerol), and the change in pK_a is accomplished without a major alteration in hydrophobicity (dioctanoyl vs dipalmitoyl). To evaluate Gro-PI as a substrate, we have applied a new assay procedure based on

Table 4: Maximal Velocities of PI-PLC Mutants toward Nonhydrophobic Substrate Analogues[a,b]

	Gro-PI	Gro-sPI
WT	1.2[c,d,g]	1.1[e,f,i]
D33A	9.2×10^{-3} [c,g,h]	0.60[e,h,i]
D33N	0.059[c,g,h]	0.82[e,h,i]
H82A	0.032[h,j]	0.67[e,h,i]

[a] Assays were performed at 25 °C. [b] Expressed in micromoles per milligram per minute. [c] Determined by the HPAEC assay method. [d] The K_m value determined for Gro-PI was 88 mM. [e] Determined by the spectrophotometric assay method. [f] The K_m value determined for Gro-sPI was 39 mM. [g] Value estimated on the basis of the velocity at a substrate concentration of 3.0 mM. [h] The V_{max} value estimated from the equation $1/V = K_m/V[S] + 1/V$, where [S] is the initial substrate concentration. The calculation was performed assuming that the K_m values for the mutant enzymes are the same as that for the WT PI-PLC. [i] Value estimated on the basis of the velocity at a substrate concentration of 3.7 mM. [j] Determined by ^{31}P NMR.

quantitation of the Gro-PI and two products of its cleavage, IcP and IP, using high-pH anion exchange chromatography (HPAEC) coupled with pulsed amperometric detection (PAD). This procedure ensures greater detection sensitivity and the use of a smaller assay volume as compared to ^{31}P NMR analysis. The activities of PI-PLC with nonhydrophobic substrates are summarized in Table 4, whereas the comparison of activities of WT PI-PLC and D33N and H82A mutants with the four substrates is illustrated in Figure 7. We have found that WT PI-PLC has very low activity toward Gro-PI with a V_{max} of 1.2 μmol min^{-1} mg^{-1} and a K_m of 88 mM. Thus, the *removal of fatty acids from the diacylglycerol moiety results in a 10^3-fold lower V_{max} and a 10^5-fold decrease in the k_{cat}/K_m ratio*. A similar result has been reported previously for mammalian PI-PLC-δ1 (*48*).

For the WT enzyme, the addition of the hydrophobic chains into the high-pK_a leaving group (Gro-PI → DPPI) resulted in the 1640-fold increase in V_{max} (Figure 7A); however, a similar action in the substrate with a low-pK_a leaving group (Gro-sPI → DOsPI) resulted only in the 43-fold activation. Furthermore, a decrease in the pK_a of the hydrophobic leaving group (DPPI → DOsPI) brought about a 34-fold reduction in V_{max}, whereas the analogous action in the nonhydrophobic leaving group (Gro-PI → Gro-sPI) did not affect at all the V_{max} value. The V_{max} decrease upon O → S substitution in the hydrophobic substrate indicates that the loss of a hydrogen bond to the leaving group due to sulfur substitution predominates over the gain in chemical reactivity due to low pK_a. Since the gain in intrinsic chemical reactivity upon O → S substitution should be similar for both hydrophobic and nonhydrophobic leaving groups, the results shown in Figure 7A suggest that hydrogen bonding stabilization of the nonhydrophobic leaving group by the enzyme is much weaker than that of the hydrophobic one.

For the D33N mutant, the effect of hydrophobic side chains in the high-pK_a leaving group is about 1 order of magnitude lower than that in the WT (187 vs 1640, Figure 7B). The most striking observation is, however, that for the D33N mutant *there is no effect of adding hydrophobic chains onto the low-pK_a leaving group* (Gro-sPI → DOsPI). On the other hand, lowering the pK_a of the hydrophobic leaving group results in a reduction in activity similar to that observed for the WT enzyme (15 vs 34), whereas lowering the pK_a in the nonhydrophobic leaving group actually *increases* the

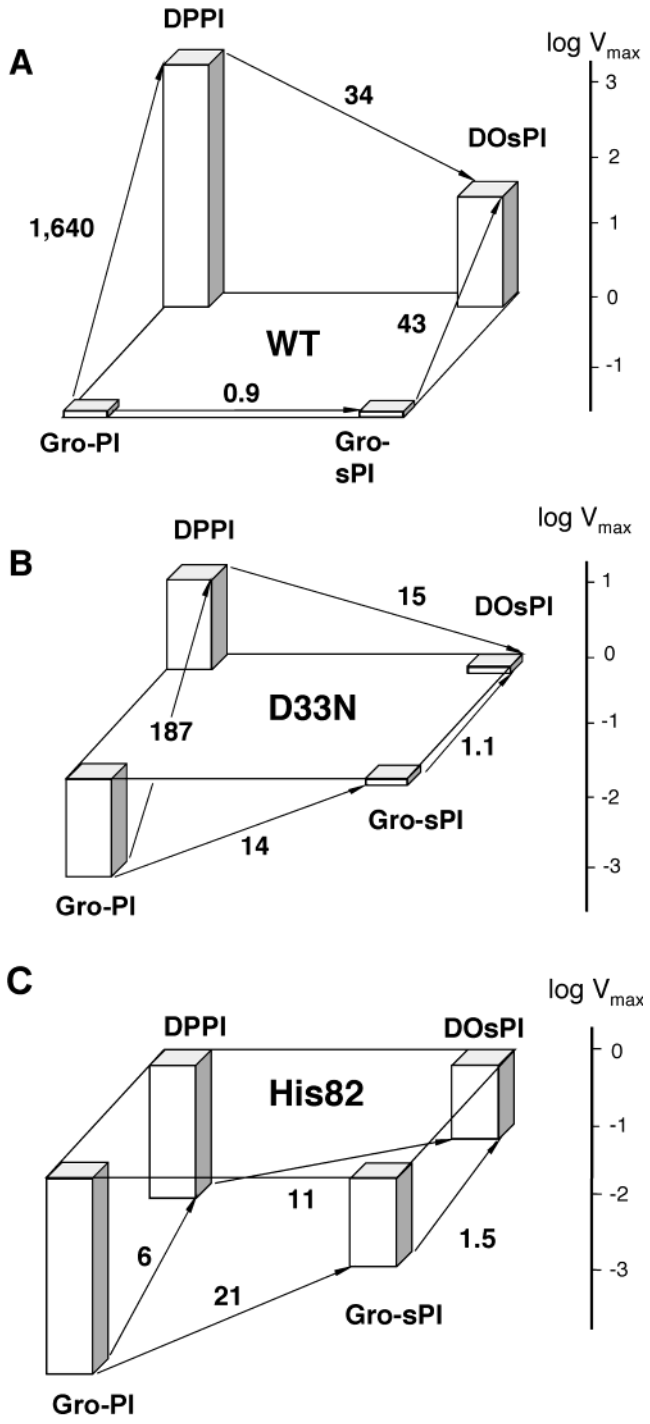

FIGURE 7: Comparison of activities of WT and mutant PI-PLC with DPPI, DOsPI, Gro-PI, and Gro-sPI: (A) WT, (B) D33N, and (C) H82A. The V_{max} values for Gro-PI and Gro-sPI were estimated as indicated in footnote h of Table 4 from the rates obtained at a substrate concentration of 3 mM. Maximum velocities are expressed in the logarithmic scale.

activity 14-fold. If it is assumed that the increase in activity due to enzyme interactions with substrate hydrophobic chains is in some way mediated by Asp33, the D33N mutant should display smaller activation, and a change to a lower-pK_a leaving group in the nonhydrophobic substrate should result in higher activity. This is what is indeed observed (Figure 7B). A similar correlation can be drawn for the H82A mutant (Figure 7C). For this mutant, however, the decrease in pK_a increases the activity even in the case of the hydrophobic

leaving group (DPPI → DOsPI), and adding the hydrophobic chains onto a substrate has a negligible effect for both low- and high-pK_a leaving groups. The interpretation of the first observation is that for this mutant in neither substrate (DPPI or DOsPI) is the leaving group activated; therefore, the pK_a has the dominant effect. Consistently, the removal of hydrophobicity from both the high- and low-pK_a leaving group brings abount no significant change in activity.

Assembly of the Arg69−Asp33−His82 Triad Is Affected by Interactions with the Hydrophobic Leaving Group. Activation of PI-PLC by the hydrophobic chains should be considered as part of an induced-fit mechanism dependent on binding of the hydrophobic leaving group. The underlying molecular mechanism has not been not understood so far; however, on the basis of kinetic studies of several active site mutants with hydrophobic and nonhydrophobic substrates performed by Gässler et al. (*14*), it is clear that the *hydrophobic interactions do not significantly alter the catalytic efficiency of the nucleophile.* This is so because mutations at His32, Asp274, and Asp198 positions bring about similar reductions in activity for both the hydrophobic (PI) and nonhydrophobic (NPIP) substrates (*14*). The results of the current work establish Asp33 and His82 as mediators through which the hydrophobic interactions between the enzyme and the substrate affect enzymatic catalysis. The most straightforward explanation is that hydrophobic interactions influence the relationship of His82 with two other members of the catalytic triad, Asp33 and Arg69. This conclusion is in agreement with structural data showing the His82 side chain located at the tip of a flexible loop (*13*). The exact positioning of the loop could be affected by hydrophobic binding.

Analogous Modes of Activation of Ribonuclease and PI-PLC by Leaving Group. It is generally accepted by enzymologists that the His119 residue of RNase A is a general acid function taking part in electrophilic assistance to the leaving group (*9*), although this notion has been disputed (*49*, *50*) on the basis of the available X-ray structures of RNase A−inhibitor complexes. In several X-ray structures, His119 occupies two alternative positions designated as A and B (*12*, *51*). Conformation A of the His119 is presumed to be catalytically competent because of the proximity of its N-H$^{\delta 2}$ hydrogen to the 5′-oxygen of the leaving group. This conformation is featured in the complex with the full substrate analogue, 2-deoxy-3′,5′-UpA, whereby binding of the adenine base causes displacement of His119 (*12*, *50*). Interestingly, in the A conformation, His119 interacts with the carboxylate group of Asp121 through its N-H$^{\epsilon 1}$ hydrogen (*51*). The kinetic advantage resulting from this interaction is much smaller in RNase A, as compared to the His82−Asp33 interaction in PI-PLC, since the D121N and D121A mutants were up only 10- and 100-fold less active, respectively, than the WT enzyme (*52*, *53*). In contrast, in both the unliganded enzyme and in its complex with 3′-UMP, His119 was found in the B position (*12*). It therefore appears that also for RNase A, the presence of the full leaving group (such as in 2-deoxy-3′,5′-UpA) is important for proper assembly of that part of the active site that catalyzes leaving group departure.

CONCLUSIONS

The observed large stereospecific thio effects of the pro-*S* nonbridging site of the WT PI-PLC and its significant reduction upon mutation of Arg69 indicate that this residue is primarily responsible for direct interaction with the pro-*S* oxygen. On the other hand, the significant reduction in the nonbridging thio effect in Asp33 mutants, as compared to WT PI-PLC, indicates that this residue is involved in interaction with Arg69. These results, along with those described earlier showing interaction of Asp33 and His82, demonstrate the presence of the unique catalytic triad composed of Arg69, Asp33, and His82. This triad is involved in both phosphate activation and protonation of the leaving group. The observed large increases in activity of the WT enzyme induced by hydrophobic chains in the high-pK_a leaving groups, and much smaller effects with lower-pK_a leaving groups indicate that the hydrophobic interactions affect catalysis of the departure of the leaving group. In addition, small effects of hydrophobicity on the activities of Asp33 and His82 mutants suggest that the hydrophobic interactions affect the assembly of the Arg69−Asp33−His82 triad.

SUPPORTING INFORMATION AVAILABLE

Description of synthetic procedures, inhibition, and PAD detector calibration data. This material is available free of charge via the Internet at http://pubs.acs.org.

REFERENCES

1. Berridge, M. J. (1993) *Nature 361*, 315−325.
2. Lin, G., Bennett, F., and Tsai, M.-D. (1990) *Biochemistry 29*, 2747−2757.
3. Bruzik, K. S., Morocho, A. M., Jhon, D.-Y., Rhee, S. G., and Tsai, M.-D. (1992) *Biochemistry 31*, 5183−5193.
4. Bruzik, K. S., and Tsai, M.-D. (1994) *Bioorg. Med. Chem. 2*, 49−72.
5. Volwerk, J. J., Shashidhar, M. S., Kuppe, A., and Griffith, O. H. (1990) *Biochemistry 29*, 8056−8062.
6. Wu, Y., Perisic, O., Williams, R. L., Katan, M., and Roberts, M. F. (1997) *Biochemistry 36*, 11223−11233.
7. Raines, R. T. (1998) *Chem. Rev. 98*, 1045−1066.
8. Messmore, J. M., Fuchs, D. N., and Raines, R. T. (1995) *J. Am. Chem. Soc. 117*, 8057−8060.
9. Thompson, J. E., and Raines, R. T. (1994) *J. Am. Chem. Soc. 116*, 5467−5468.
10. Herschlag, D. J. (1994) *J. Am. Chem. Soc. 116*, 11631−11635.
11. Gerlt, J. A., and Gassman, P. G. (1993) *Biochemistry 32*, 11943−11952.
12. Zegers, I., Maes, D., Dao-Thi, M.-H., Poortmans, F., Palmer, R., and Wyns, L. (1994) *Protein Sci. 3*, 2322−2339.
13. Heinz, D. W., Ryan, M., Bullock, T. L., and Griffith, O. H. (1995) *EMBO J. 14*, 3855−3863.
14. Gässler, C. S., Ryan, M., Liu, T., Griffith, O. H., and Heinz, D. W. (1997) *Biochemistry 36*, 12802−12813.
15. Hondal, R. J., Zhao, Z., Kravchuk, A. V., Liao, H., Riddle, S. R., Yue, X., Bruzik, K. S., and Tsai, M.-D. (1998) *Biochemistry 37*, 4568−4580.
16. Hondal, R. J., Bruzik, K. S., and Tsai, M.-D. (1997) *J. Am. Chem. Soc. 119*, 9933−9934.
17. Moser, J., Gerstel, B., Meyer, J. E. W., Chakraborty, T., Wehland, J., and Heinz, D. W. (1997) *J. Mol. Biol. 273*, 269−282.
18. Liu, T., Ryan, M., Dahlquist, F. W., and Griffith, O. H. (1999) *ACS Symp. Ser. 718*, 91−108.
19. Hondal, R. J., Bruzik, K. S., Zhao, Z., and Tsai, M.-D. (1997) *J. Am. Chem. Soc. 119*, 5477−5478.

20. Burgers, M. J., and Eckstein, F. (1979) *Biochemistry 18*, 592−596.
21. Eckstein, F. (1970) *J. Am. Chem. Soc. 92*, 4718−4723.
22. Hondal, R. J., Riddle, R. R., Kravchuk, A. V., Zhao, Z., Bruzik, K. S., and Tsai, M.-D. (1997) *Biochemistry 36*, 6633−6642.
23. Kubiak, R. J., Hondal, R. J., Yue, X., Tsai, M.-D., and Bruzik, K. S. (1999) *J. Am. Chem. Soc. 121*, 488−489.
24. Hondal, R. J., Zhao, Z., Kravchuk, A. V., Riddle, S. R., Bruzik, K. S., and Tsai, M.-D. (1998) *ACS Symp. Ser. 718*, 180−196.
25. Mihai, C., Mataka, J., Riddle, S., Tsai, M.-D., and Bruzik, K. S. (1997) *Bioorg. Med. Chem. Lett. 7*, 1235−1238.
26. Bruzik, K. S., Hakeem, A. A., and Tsai, M.-D. (1994) *Biochemistry 33*, 8367−8374.
27. Leigh, A. J., Volwerk, J. J., Griffith, O. H., and Keana, J. F. W. (1992) *Biochemistry 31*, 8978−8983.
28. Hendrickson, E. K., Hendrickson, H. S., Johnson, J. L., Khan, T. H., and Chial, H. J. (1992) *Biochemistry 31*, 12169−12172.
29. Kuteladze, T. G., Scuster, M. C., Venegas, F. D., Messmore, J. M., and Raines, R. T. (1995) *Bioorg. Chem. 23*, 471−481.
30. Hollfelder, F., and Herschlag, D. (1995) *Biochemistry 34*, 12255−12264.
31. Volwerk, J. J., Filhuth, E., Griffith, O. H., and Jain, M. K. (1994) *Biochemistry 33*, 3364−3474.
32. Zhang, Y.-L., Hollfelder, F., Gordon, S. J., Chen, L., Keng, Y.-F., Wu, L., Herschlag, D., and Zhang, Z.-Y. (1999) *Biochemistry 38*, 12111−12125.
33. Martin, S. F., and Wagman, A. S. (1996) *J. Org. Chem. 61*, 8016−8023.
34. Kravchuk, A. V., Zhao, L., Kubiak, R. J., Bruzik, K. S., and Tsai, M.-D. (2001) *Biochemistry 40*, 5433−5439.
35. Baraniak, J., and Frey, P. A. (1988) *J. Am. Chem. Soc. 110*, 4059−4060.
36. Frey, P. A., Reimschüssel, W., and Paneth, P. (1986) *J. Am. Chem. Soc. 108*, 1720−1721.
37. Oivanen, M., Ora, M., Almer, H., Stromberg, R., and Lonnberg, H. (1995) *J. Org. Chem. 60*, 5620−5627.
38. Kubiak, R. J., and Bruzik, K. S. (2001) *J. Am. Chem. Soc. 123*, 1760−1761.
39. Eckstein, F. (1968) *FEBS Lett. 2*, 85−86.
40. Davis, A. M., Hall, A. D., and Williams, A. (1988) *J. Am. Chem. Soc. 110*, 5105−5108.
41. Bruice, T. C., and Benkovic, S. J. (2000) *Biochemistry 39*, 6267−6274.
42. Carter, P., and Wells, J. A. (1988) *Nature 332*, 6164.
43. Beveridge, A. J. (1996) *Protein Sci. 5*, 1355−1365.
44. Rink, R., Fennema, M., Smids, M., Dehmel, U., and Janssen, D. B. (1997) *J. Biol. Chem. 272*, 14650−14657.
45. Chen, P., Tsuge, H., Almassy, R. J., Gribskov, C. L., Katoh, S., Vanderpool, D. L., Margosiak, S. A., Pinko, C., and Matthews, D. A. (1996) *Cell 86*, 835−843.
46. Shashidhar, M. S., Volwerk, J. J., Griffith, O. H., and Keana, J. F. W. (1991) *Chem. Phys. Lipids 60*, 101−110.
47. Zhou, C., Wu, Y., and Roberts, M. F. (1997) *Biochemistry 36*, 347−355.
48. Wu, Y., Perisic, O., Williams, R. L., Katan, M., and Roberts, M. F. (1997) *Biochemistry 36*, 11223−11233.
49. Lim, C., and Tole, P. (1992) *J. Am. Chem. Soc. 114*, 7245−7252.
50. Breslow, R., Huang, D.-L., and Anslyn, E. (1989) *Proc. Natl. Acad. Sci. U.S.A. 86*, 1746−1750.
51. Toiron, C., Gonzalez, C., Bruix, M., and Rico, M. (1996) *Protein Sci. 5*, 1633−1647.
52. Trautwein, K., Holliger, P., Stackhouse, J., and Benner, S. A. (1991) *FEBS Lett. 281*, 275−277.
53. Schultz, L. W., Quirk, D. J., and Raines, R. T. (1998) *Biochemistry 37*, 8886−8898.
54. Griffith, O. H., and Ryan, M. (1999) *Biochim. Biophys. Acta 1441*, 237−254.

BI002371Y